Method for In Situ Film Thickness Measurement of Ball Bearings under Combined Loading using Capacitance Measurements

Volker Schneider[a], Norbert Bader[a], Haichao Liu[a] and Gerhard Poll[a]

[a] *Institute of Machine Design and Tribology, Leibniz University Hannover, 30823 Garbsen*

ARTICLE INFO

Keywords:
Film Thickness
Condition Monitoring
Capacitance Method
Rolling Bearing

ABSTRACT

In this study, a novel capacitance based analytical method to monitor the film thickness in a ball bearing under a combination of axial and radial load is presented. Furthermore, an extended method is presented to infer the difference between the lubricant film height on the inner ring and the outer ring of a rolling element. Numerical investigations provide the basis for describing the influence of the operating parameters on the lubricant film thickness distribution in the HERTZ'ian contact. The method for calculating the correction factor k_c presented in a previous paper is extended so that it is valid for a wider operating range. This makes it possible to calculate the total capacitance of a contact from the capacitance of only the HERTZ'ian contact area.

1. Introduction

Knowledge of the lubricating film thickness in a rolling contact is fundamental for understanding the hydrodynamic rolling friction in EHL-regime as well as an important parameter influencing electrical bearing load. In systems where an electrical potential is present on the inner or outer bearing ring, voltage breakdown can occur. The film thickness has a great influence on the severity of the electrical damage, since it affects the breakdown-threshold. When looking at electric-motor bearings the film thickness and therefore the capacitance have an effect on the voltage divider (Bearing Voltage Ratio - BVR), which defines the magnitude of the common-mode-voltage that is present in the bearing. The BVR consists of motor and bearing capacitances and was introduced by MÜTZE [1]. To predict the bearing voltage and EDM current, knowledge about the capacitances of both a single EHL contact and a whole bearing are required.

The capacitance of a model EHL contact can be determined by assuming the EHL contact as a plate capacitor with capacitance:

$$C = \epsilon \cdot \frac{A}{d_{\mathrm{gap}}} \tag{1}$$

where $\epsilon = \epsilon_0 \cdot \epsilon_r$ is the absolute permittivity of the dielectric in an EHL contact, where ϵ_0 is the permittivity of vacuum and ϵ_r is the relative permittivity of the dielectric, A is the contact area, and d_{gap} is the film thickness of the HERTZ'ian contact zone. In addition, the influence of the regions outside the HERTZ'ian contact zone on the capacitance C_{outside} must be taken into account (see Figure 1) [2, 3, 4, 5, 6, 7, 8].

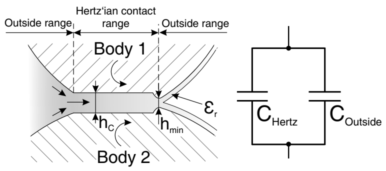

Figure 1: *Electrical analogy model of an EHL contact.*

The total capacitance of a contact $C_{\mathrm{tot,con}}$ is then a sum of C_{Hertz} and C_{Outside}. C_{Hertz} may be approximated by

$$C_{\mathrm{Hertz,h_c}} = \epsilon_0 \cdot \epsilon_r \cdot \frac{A_{\mathrm{Hertz}}}{h_c} \tag{2}$$

Nomenclature

Greek Symbols

α	operating contact angle	rad
α_p	pressure-viscosity coefficient	Pa^{-1}
$\alpha_{nominal}$	nominal contact angle	rad
Δt	time difference between two voltage limits	s
δ	deflection	m
ϵ	absolute permittivity	F/m
ϵ_0	vacuum permittivity = 8.8541878×10^{-12} A s/V m	
ϵ_r	relative permittivity	–
η_0	dynamic viscosity U	mPa s
γ	tilt angle	rad
ν	POISSON's ratio	–
Ψ	azimuth angle of rolling element	rad
ρ	curvature	1/m
τ	time constant	s

Roman Symbols

$\bar{v}$	entrainment velocity	m/s
$\mathcal{E}$	complete elliptical integral of second order	–
$\mathcal{F}$	complete elliptical integral of first order	–
A	area	m^2
a	distance between raceway groove curvature centers	m
a	greater half-width of contact ellipse	m
b	lesser half-width of contact ellipse	m
C	capacitance	F
d_{gap}	thickness of gap between capacitor plates	m
d_{groove}	raceway groove diameter	m
d_{ref}	pitch diameter	m
d_{re}	ball diameter	m
E	elastic modulus	Pa
E'	equivalent elastic modulus	Pa
F	force	N
G	dimensionless material parameter	–
H	dimensionless film thickness	–
h	film thickness	m
k_c	ratio between C_{total} and C_{Hertz,h_c}	–
k_e	ellipticity ratio $k = \frac{a}{b}$	–
k_h	ratio between h_o and h_i	–
K_p	load-deflection factor	$N/m^{3/2}$
k_Q	capacitance proportionality factor	–
M	load torque	Nm
n	rotational speed	1/min
P_d	radial clearance	m
Q	contact load	N
R	composite radius	m
r	radius	m
R_L	charging resistance	Ω
R_P	parallel resistance	Ω
$r_{p,q}$	distance of raceway groove curvature centers to the rotational axis	m
$R_{y,Q}$	osculation	-
U	dimensionless speed parameter	–
U	voltage	V
W	dimensionless load parameter	–
Z	number of rolling elements	–

Subscripts

$brng$	bearing
c	central
con	contact
i	inner raceway
j	j^{th} rolling element
o	outer raceway
re	rolling element
rs	replenishment/starvation
th	thermal
tot	total
x	x-direction
y	y-direction

assuming the film thickness inside the HERTZ'ian contact zone being equal to the central film thickness h_c, which can be calculated from analytical equations. A suitable set of equations for point contacts is provided by e.g. HAMROCK and DOWSON [9]. The equations are based on a set of dimensionless parameters for speed U, material G, load W and ellipticity k_e (see Equation 3, with Eqs. 17 - 19).

$$H_c = \frac{h_c}{R_x} = 2.69 \cdot G^{0.530} \cdot U^{0.67} \cdot W^{-0.067} \cdot (1 - 0.61 \cdot e^{-0.73 \cdot k_e}) \tag{3}$$

Additional influences on the film thickness need to be considered, an explanation is given in the former work of the authors [10]. This includes:

- Temperature rise as a result of reverse flow in the inlet zone based on the work of MURCH-WILSON [11]. This leads to a reduced film thickness as a result of a lower viscosity.
- Starvation influence as a result of insufficient time for the lubricant to flow back into contact after an overrolling based on [12].
- Influence of surface roughness on EHL film formation [13].

For film thickness measurement, the knowledge of the influence of the real EHL film shape on the total capacitance is of great importance. However, in literature this was usually simplified by assuming a uniform thickness of h_c [14, 7, 8, 15, 16, 5, 17]. To describe the influence of the realistic film shape and the regions outside the HERTZ'ian contact a factor k_C was introduced, which describes the ratio between the total contact capacitance $C_{tot,con}$ and the capacitance of the HERTZ'ian contact area with a uniform film thickness C_{Hertz,h_c}. By comparing the measured capacitances in bearing tests with calculated capacitances according to EHL theory, BARZ [4] determined the k_c factor for the considered case with axially loaded spindle bearings to be a uniform value of $k_c = 3.5$. This gives a relatively good approximation for the investigated axially loaded ball bearings and was also used by WITTEK ET AL. [17]. However, the capacitance surrounding the HERTZ'ian contact $C_{outside}$ is a function of film thickness as shown in the work of JABLONKA ET AL. [5] and in the former work of the authors [10], in which the influence of a realistic film thickness distribution on the total contact capacitance was described and a formula to calculate the k_c factor was derived. The formula is based only on the HAMROCK-DOWSON group of dimensionless parameters for film thickness calculation.

$$k_C(U, G, W, k_e) = \frac{C_{tot,con}}{C_{Hertz,h_c}} \tag{4}$$

The total capacitance of one contact including the influence of a realistic film thickness distribution and the region surrounding the Hertzian contact is then an extension of Equation 2 and calculated as follows

$$C_{tot,con} = \epsilon_0 \cdot \epsilon_r \cdot k_c(U, G, W, k_e) \cdot \frac{A_{Hertz}(F_N, R, E')}{h_c(\bar{v}, F_N, R, E', \eta)} \tag{5}$$

The capacitance of the inner and outer ring contact are in series. In order to calculate the capacitance of the j^{th} rolling element both proportions add up as

$$C_{j,re,calc} = \frac{C_{tot,con,IR,i} \cdot C_{tot,con,OR,i}}{C_{tot,con,IR,i} + C_{tot,con,OR,i}} \tag{6}$$

To calculate the capacitance of the whole bearing $C_{bearing,tot}$ with Z rolling elements in parallel, the capacitances for each rolling element need to be added up.

$$C_{bearing,total} = \sum_{j=1}^{Z} C_{j,re,calc} \tag{7}$$

This work will present a method to calculate the film thickness in a combined loaded ball bearing. This method is an extension of existing electrical capacitance methods developed in e.g., [5, 6, 14, 18, 19, 20, 21, 22] and could help to monitor the film thickness in bearing applications. The basis of this is the measurement of the rolling bearing capacitance C_{total} during operation (see Sec. 2). To conclude from the total capacitance C_{total} to the individual capacitances of each rolling element a factor k_Q is introduced and used in combination with the k_C factor. To further distinguish between the capacitance of the inner and outer ring contact a factor k_h is utilized. An analytical equation was derived for each factor and the relationship of these is explained in an application example based on measured values. The following is a brief description of the derived equations and a reference to the associated sections.

Relation between the total capacitance and the individual capacitances per contact with k_Q-Factor (Equation 41)
A factor k_Q is introduced to describe the relationship between the capacitance of a single contact and the total capacitance in a combined loaded bearing. The factor provides the possibility to infer the single contact capacitance from the measured C_{total} based only on the calculable internal load distribution (see Sec. 3.2).

Empirical Equation of k_h-Factor (Equation 44)
The k_h-factor describes the relation between the film thickness of the inner and outer ring contact and was originally introduced by BARZ [4]. This study presents an empirical equation to describe k_h as a function of the geometries based on the work of HAMROCK and DOWSON [9] (see Sec. 3.3).

Extension of k_c-Factor (Equation 16)
The factor $k_c(U, G, W, k_e)$ expresses the ratio between the HERTZ'ian zone capacitance and the total contact capacitance as described e.g., in [16, 22, 23]. The factor presented from the authors [10] is extended and fitted to higher loads (parameter W) and a wider range of osculations (parameter k_e) (see Sec. 2.3).

In order to determine the mentioned factors, EHL contact capacitances for different speeds, materials and loads have been determined both analytically and numerically. The approaches are explained in detail in the following sections. The proposed formulae have been applied to analytical capacitance calculations for rolling element bearings under combined load conditions. Capacitance measurements of a rolling bearing have been carried out for comparison and validation of the proposed factors.

2. Film Thickness Measurement for Axially Loaded Bearings

With the capacitance measurement, a quantitative film thickness determination is possible. This makes use of the fact that the contact under full-film lubrication can be seen as a capacitor due to the two surfaces separated by a dielectric (between rolling element and raceway).

2.1. State of the art of capacitance determination with voltage measurement

When a voltage step U_0 is applied to a capacitor, the system charging response can be measured and the capacitance of a single contact or a rolling bearing can be deduced from the typical charging behavior of the capacitor [2, 4, 22]. To charge the capacitor a limited charging current is needed. This is realized using a known charging resistance R_L (see Figure 2), which is connected in series to the capacitance. Additionally an ohmic resistance R_P parallel to the capacitor needs to be considered, which is caused by the lubricant specific ohmic resistance. This value isn't known initially and needs to be calculated from the system response (see Equation 11). If the parallel resistance R_P isn't infinitely large, the maximum measurable voltage U_{max} of a fully charged capacitor is lower than the charging voltage U_0. To calculate the capacitance the time constant τ is used.

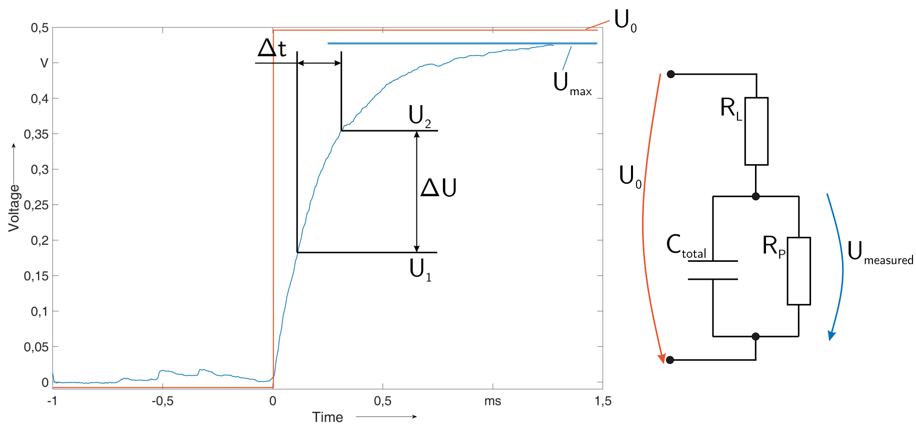

Figure 2: *Determination of time constant τ from measured charging behaviour.*

The capacitance is then calculated by the evaluation of the time constant and the following correlation of the charging characteristic.

$$C_{\mathrm{tot}} = \tau \cdot \left(\frac{1}{R_{\mathrm{L}}} + \frac{1}{R_{\mathrm{P}}} \right) \tag{8}$$

where

$$\tau = \frac{\Delta t}{ln\left(1 - \frac{U_1}{U_{\mathrm{max}}}\right) - ln\left(1 - \frac{U_2}{U_{\mathrm{max}}}\right)} \tag{9}$$

$$U_{\mathrm{measured}} = U_0 \cdot (1 - e^{-\frac{t}{\tau}}) \tag{10}$$

$$R_{\mathrm{P}} = R_{\mathrm{L}} \cdot \left(\frac{U_{\mathrm{max}}}{U_0 - U_{\mathrm{max}}} \right) \tag{11}$$

2.2. State of the art of film thickness calculation with measured capacitance

When there is only an axial load, the contact loads are equal among the Z rolling elements. If the same film thickness is present on the inner and outer ring, the film thickness can be calculated as follows.

$$h_{\mathrm{measured,simplified}} = \frac{1}{2} \cdot \frac{Z \cdot k_{\mathrm{C}} \cdot \epsilon_0 \cdot \epsilon_{\mathrm{r}} \cdot A_{\mathrm{Hertz}}}{C_{\mathrm{tot}}} \tag{12}$$

However, due to the different geometries of the inner/outer ring contact, the film thickness is not identical, therefore BARZ [4] introduced a proportionality factor k_{h}, which describes the ratio of the film thickness between the inner and outer ring contact. It can be calculated based on the analytical HAMROCK-DOWSON EHL-Equations.

$$k_{\mathrm{h}} = \frac{h_{\mathrm{o}}}{h_{\mathrm{i}}} \equiv \frac{h_{\mathrm{measured,o}}}{h_{\mathrm{measured,i}}} \equiv \frac{h_{\mathrm{EHL,o}}}{h_{\mathrm{EHL,i}}} \tag{13}$$

If this ratio is used to determine the film thickness on the inner ring, the formula for the calculation is as follows, by still assuming uniform load distribution in the bearing and using the same k_{C} factor for all contacts

$$h_{\mathrm{measurement,i}} \approx Z \cdot k_{\mathrm{C}} \cdot \epsilon_0 \cdot \frac{(\epsilon_{\mathrm{r,i}} \cdot A_{\mathrm{Hertz,i}}) \cdot \left(\epsilon_{\mathrm{r,o}} \cdot \frac{A_{\mathrm{Hertz,o}}}{k_{\mathrm{h}}}\right)}{(\epsilon_{\mathrm{r,i}} \cdot A_{\mathrm{Hertz,i}}) + \left(\epsilon_{\mathrm{r,o}} \cdot \frac{A_{\mathrm{Hertz,o}}}{k_{\mathrm{h}}}\right)} \cdot \frac{1}{C_{\mathrm{tot}}} \tag{14}$$

and on the outer ring by

$$h_{\mathrm{measurement,o}} \approx k_{\mathrm{h}} \cdot h_{\mathrm{measurement,i}} \tag{15}$$

These formulae do not cover the case when the internal load is unevenly distributed among the rolling elements. Beginning from section 3, it is discussed how the existing approaches can be extended so that complex load cases can be calculated as well.

Table 1
Valid range of dimensionless parameters for the determined k_C-factor.

Parameter	Variation range from [10]	Extended Variation range
U	$0.56...22.52 \cdot 10^{-11}$	$0.56...22.52 \cdot 10^{-11}$
G	3300...4615.4	3300...4615.4
W	$3.44...289.58 \cdot 10^{-6}$	$3.44...573.3 \cdot 10^{-6}$
k_e	3.125...7.878	3.125...11.713

2.3. Extension of factor k_C

As shown in Figure 1, it is necessary to know the capacitance of the regions surrounding the HERTZ'ian contact zone, in order to derive the film thickness from a measured capacitance. Since available methods only covered a specific load case [4, 22] or required a large experimental base [16], the authors presented an empirical factor in a previous work [10] that allowed to infer the total capacitance of a contact from the easily calculable HERTZ'ian capacitance, using only the dimensionless parameters U, G, W, k_e.
The obtained equation for the influence factor k_C represents a curve fit of simulation results, that were conducted with an EHL solver, that has been introduced by LUBRECHT and VENNER [24, 25]. It is based on the multigrid-method to solve the coupled Reynolds equation, which takes the surface elastic deformation and load balance into account. In comparison to the previous factor, additional simulations have been conducted in this work to extend the load factor W and the ellipticity parameter k_e, to cover higher load applications and longer HERTZ'ian contacts (by means of larger half-width a) to cover a broader range of osculations. To find fitted exponents of a derived equation based on the set of nonlinear parameters, the LEVENBERG-MARQUARDT algorithm [26, 27] from the MATLAB *fsolve* function was used. The obtained Equation 16 has a first-order optimality of $2.78e-4$.
A comparison between the previous and the extended simulation variation range is given in Table 1 and a general overview of the valid parameter range for the conducted simulations is displayed in Figure 3. Please note that the bounding boxes have been drawn on the graphic for illustrative purposes only, to guide the reader's eye.

$$k_C(U, G, W, k_e) = 6.9116 \cdot U^{0.2675} \cdot W^{-0.2768} \cdot G^{0.2599} \cdot k_e^{0.1033} \tag{16}$$

with

$$U = \frac{\eta_0 \bar{v}}{E' R_x} \tag{17}$$

$$G = \alpha_p E' \tag{18}$$

$$W = \frac{Q}{E' R_x^2} \tag{19}$$

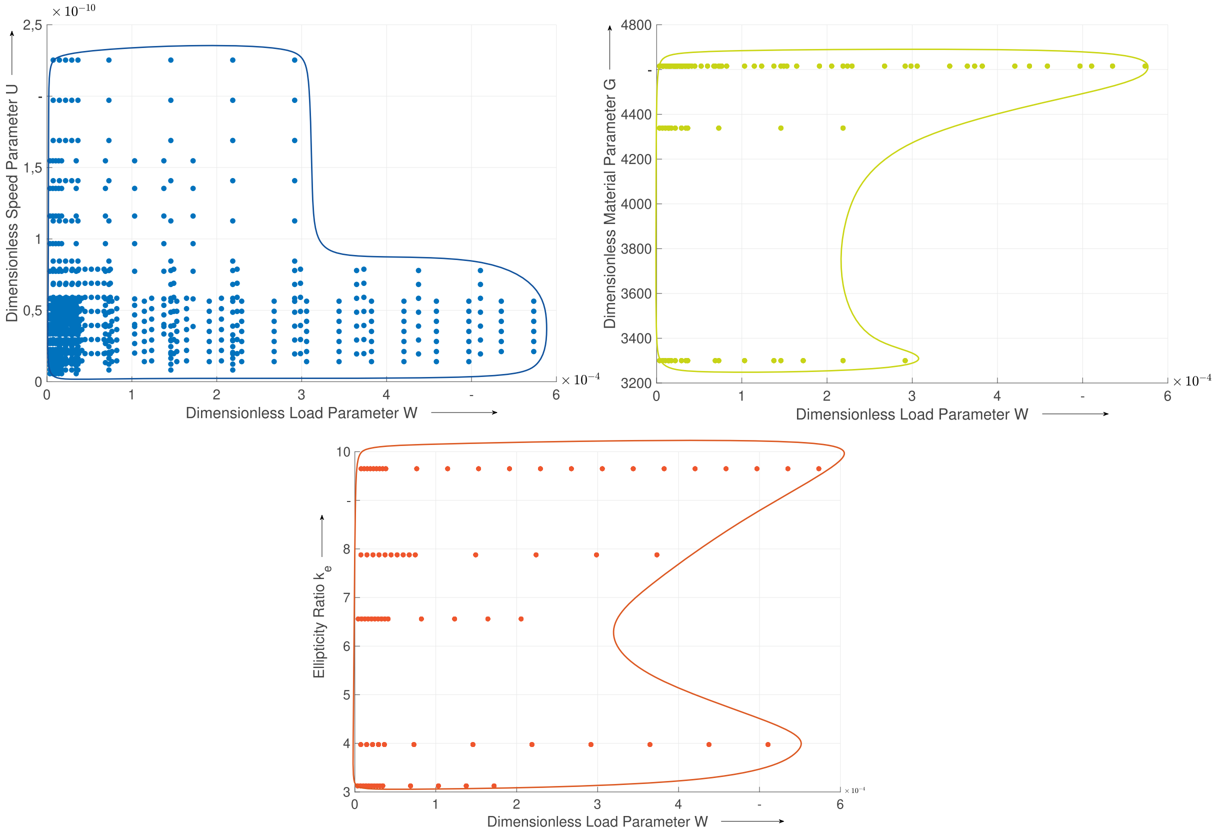

Figure 3: *Valid areas of dimensionless parameters for the determined k_C-factor.*

For validation of the newly derived k_C factor a comparison was made between capacitance measurements by FURTMANN [16] and capacitance calculations using the previous k_C factor from [10] and the newly extended k_C factor (see Figure 4 and 5). Compared to the previous factor an improvement in the capacitance calculation was achieved. The hatched area in the combined load case represents the influence of the theoretical range of operating clearance, which is influenced by the the tolerances and the temperature in the system. Specifically this refers to the tolerances of shaft-, and housing-fits, as well as the bearing internal clearance class. A theoretical minimum operating clearance of -9 µm and a maximum of $+16$ µm were considered.

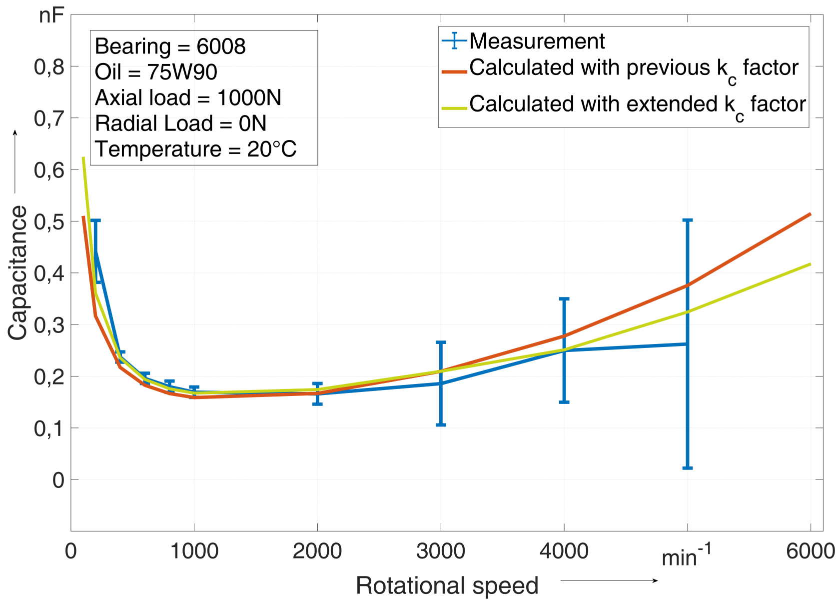

Figure 4: *Comparison of capacitance measurements from* FURTMANN *[16] with capacitance calculations, using the previous k_C factor from [10] and the newly extended k_C factor. Pure axial load case.*

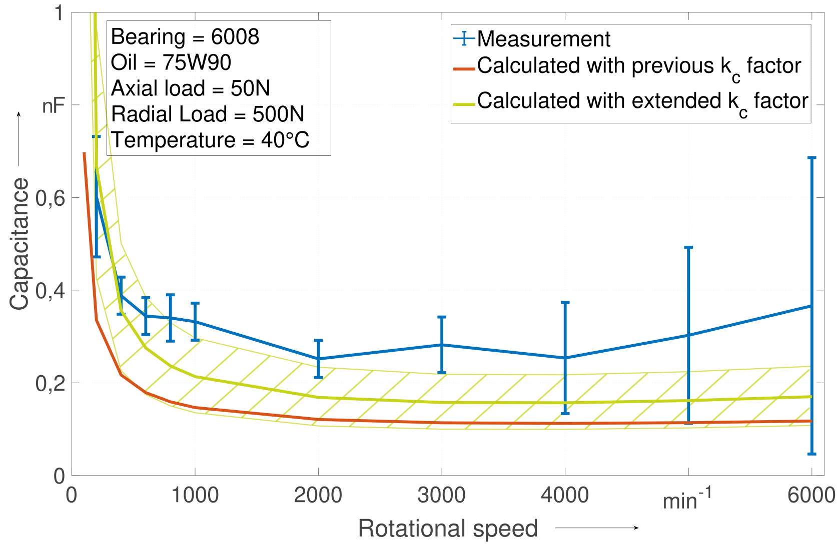

Figure 5: *Comparison of capacitance measurements from* FURTMANN *[16] with capacitance calculations, using the previous k_C factor from [10] and the newly extended k_C factor. The hatched area shows the capacitance range with variation of the operating clearance. Combined load case.*

3. Extension of Film Thickness Formulae to Combined Load Cases

Due to weight forces and/or additionally applied radial load, the resulting film thickness is no longer uniformly distributed over the contacts of the bearing. Thus, we introduce a proportionality factor k_Q, which is the ratio between the combined capacitance of one rolling element (rolling element-inner ring contact and the -outer ring contact) and the total capacitance:

$$C_{\mathrm{tot}} = \sum_{\mathrm{j=1}}^{Z} k_{\mathrm{Q,j}} \cdot C_{\mathrm{total}} = \sum_{\mathrm{j=1}}^{Z} C_{\mathrm{re,j}} = \sum_{\mathrm{j=1}}^{Z} \frac{C_{\mathrm{i,j}} \cdot C_{\mathrm{o,j}}}{C_{\mathrm{i,j}} + C_{\mathrm{o,j}}} \tag{20}$$

with the calculated capacitance of one rolling element $C_{\mathrm{j,re,calc}}$ and the calculated total capacitance of the bearing $C_{\mathrm{bearing,tot,calc}}$ (see Eqs. 6 and 7) the proportionality factor k_{Q} depending on the capacitance results to

$$k_{\mathrm{Q,j,calc}}(C) = \frac{C_{\mathrm{j,re,calc}}}{C_{\mathrm{bearing,tot,calc}}} \tag{21}$$

Assuming that the factor k_{Q} is known and using a more precise k_{C} factor for the inner and outer ring contact, the film thickness of the j^{th} rolling element with measured total capacitance $C_{\mathrm{tot,measured}}$ on the inner ring is calculated according to Equation 22

$$h_{\mathrm{measured,i,j}} = \epsilon_0 \cdot \frac{(k_{\mathrm{C,i}} \cdot \epsilon_{\mathrm{r,i}} \cdot A_{\mathrm{Hertz,i}}) \cdot \left(k_{\mathrm{C,o}} \cdot \epsilon_{\mathrm{r,o}} \cdot \frac{A_{\mathrm{Hertz,o}}}{k_{\mathrm{h}}}\right)}{(k_{\mathrm{C,i}} \cdot \epsilon_{\mathrm{r,i}} \cdot A_{\mathrm{Hertz,i}}) + \left(k_{\mathrm{C,o}} \cdot \epsilon_{\mathrm{r,o}} \cdot \frac{A_{\mathrm{Hertz,o}}}{k_{\mathrm{h}}}\right)} \cdot \frac{1}{C_{\mathrm{tot,measured}} \cdot k_{\mathrm{Q,j}}} \tag{22}$$

where

$$k_{\mathrm{C,i/o}} = f(U, G, W, k_{\mathrm{e}}) \tag{23}$$

Since it is relatively complex to calculate the individual and total capacitances of a bearing (see the former work of the authors [10]), the aim is to describe the factor k_{Q} with more easily calculable values in order to derive the film thicknesses in a bearing under combined load. The presented methods are based on calculations for normal operating speeds. Therefore, the following simplifications can be made for the determination of the aforementioned factors:

- the bearing is mounted on a sturdy shaft and in a rigid housing;
- the bearing components are assumed to be rigid except the local contact zones;
- the contact angle under the operational parameters are equal for the inner and outer ring contact;
- centrifugal forces are neglected.

Looking only at the operational parameters within one bearing, material and speed are almost constant at each rolling element, even at different contact angles. When comparing different bearing sizes, the significant difference is the geometry, more specifically the osculation between the rolling element and the raceway. To develop a generally valid formula, the relationship among load, osculation and capacitance distribution needs to be built. The load distribution on which the calculation is based has to be described firstly.

3.1. Load distribution

In order to calculate the equilibrium of forces and moments, the five degrees of freedom approach presented by Andreason [28] is used. With the definition of the coordinate system shown in Figure 6 a) and Figure 6 b) the equilibrium to be established is:

$$\left.\begin{aligned}
0 &= F_{\mathrm{x}} - \sum_{\mathrm{j}=1}^{Z} Q_{\mathrm{j}} \cdot \cos\alpha_{\mathrm{j}} \cdot \cos\psi \\
0 &= F_{\mathrm{y}} - \sum_{\mathrm{j}=1}^{Z} Q_{\mathrm{j}} \cdot \cos\alpha_{\mathrm{j}} \cdot \sin\psi \\
0 &= F_{\mathrm{z}} - \sum_{\mathrm{j}=1}^{Z} Q_{\mathrm{j}} \cdot \sin\alpha_{\mathrm{j}} \\
0 &= M_{\mathrm{x}} - r_{\mathrm{q}} \cdot \sum_{\mathrm{j}=1}^{Z} Q_{\mathrm{j}} \cdot \sin\alpha_{\mathrm{j}} \cdot \sin\psi \\
0 &= M_{\mathrm{y}} + r_{\mathrm{q}} \cdot \sum_{\mathrm{j}=1}^{Z} Q_{\mathrm{j}} \cdot \sin\alpha_{\mathrm{j}} \cdot \cos\psi
\end{aligned}\right\} \tag{24}$$

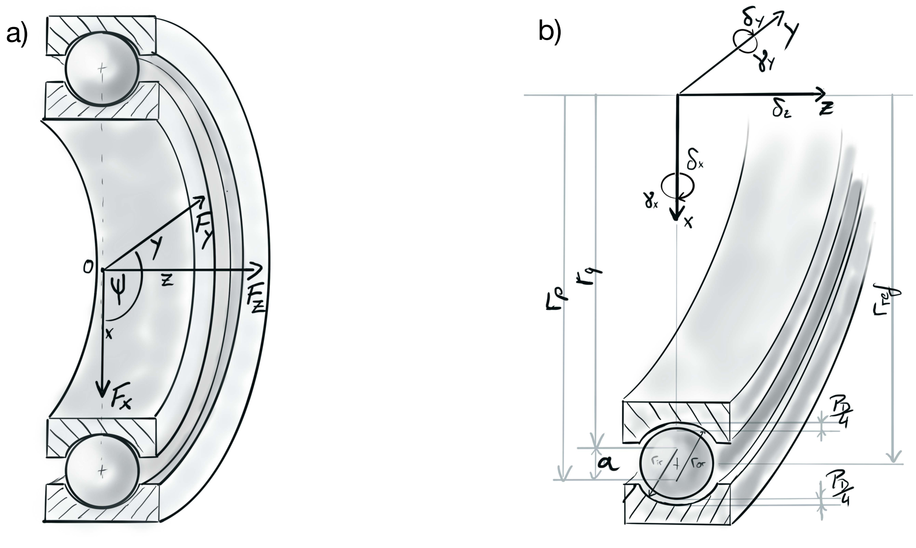

Figure 6: *a) Coordinate system and angles, b) Deflections, tilting angles as well as general geometries*

With a contact angle of the j^{th} rolling element

$$\alpha_{\mathrm{j}} = \tan^{-1}\left(\frac{\delta_{\mathrm{z}} + r_{\mathrm{p}} \cdot (\gamma_{\mathrm{x}} \cdot \sin\psi_{\mathrm{j}} - \gamma_{\mathrm{y}} \cdot \cos\psi_{\mathrm{j}})}{\delta_{\mathrm{x}} \cdot \cos\psi_{\mathrm{j}} + \delta_{\mathrm{y}} \cdot \sin\psi_{\mathrm{j}} + a}\right) \tag{25}$$

The load-deformation relation was not adopted from ANDREASON but extended using the approach from HAMROCK and DOWSON [9] so that there is no need to rely on a look up table for different osculations.

$$Q_{\mathrm{j}} = K_{\mathrm{p}} \cdot \delta_{\mathrm{total,j}}^{1.5} = Q_{\mathrm{i,j}} = Q_{\mathrm{o,j}} \tag{26}$$

The total deflection of the j^{th} rolling element $\delta_{\mathrm{total,j}}$ is calculated as follows

$$\delta_{\mathrm{total,j}} = \frac{\delta_{\mathrm{x}} \cdot \cos\psi_{\mathrm{j}} + \delta_{\mathrm{y}} \cdot \sin\psi_{\mathrm{j}} + a}{\cos\alpha_{\mathrm{j}}} - a - \frac{P_{\mathrm{d}}}{2} \tag{27}$$

with

$$\begin{aligned} &0 < \delta_{\text{total}} \\ &a = r_{\text{p}} - r_{\text{q}} \\ &r_{\text{p}} = \frac{d_{\text{ref}}}{2} - \frac{d_{\text{re}}}{2} - \frac{P_{\text{d}}}{4} + \frac{d_{\text{i,groove}}}{2} \\ &r_{\text{q}} = \frac{d_{\text{ref}}}{2} + \frac{d_{\text{re}}}{2} + \frac{P_{\text{d}}}{4} - \frac{d_{\text{o,groove}}}{2} \end{aligned} \tag{28}$$

and the load deflection as a function of the given geometric relations is

$$K_{\text{p}} = \frac{1}{\left(\left(\frac{1}{K_{\text{p,i}}}\right)^{\frac{2}{3}} + \left(\frac{1}{K_{\text{p,o}}}\right)^{\frac{2}{3}}\right)^{1.5}} \tag{29}$$

$$K_{\text{p,i/o}} = \pi \cdot \bar{k}_{\text{e}} \cdot E' \left(\frac{\sum \rho \cdot \bar{\mathcal{E}}}{4.5 \cdot \bar{\mathcal{F}}}\right) \tag{30}$$

$$\sum \rho = \frac{1}{R} \tag{31}$$

$$\frac{1}{R} = \frac{1}{R_{\text{x}}} + \frac{1}{R_{\text{y}}} = \frac{1}{r_{\text{x,1}}} + \frac{1}{r_{\text{x,2}}} + \frac{1}{r_{\text{y,1}}} + \frac{1}{r_{\text{y,2}}} \tag{32}$$

$$\bar{k}_{\text{e}} = 1.0339 \cdot \left(\frac{R_{\text{y}}}{R_{\text{x}}}\right)^{0.636} \tag{33}$$

$$\bar{\mathcal{F}} = 1.5277 + 0.6023 \cdot \ln \frac{R_{\text{y}}}{R_{\text{x}}} \tag{34}$$

$$\bar{\mathcal{E}} = 1.0003 + \frac{0.5968}{R_{\text{y}}/R_{\text{x}}} \tag{35}$$

$$E' = 2\left(\frac{1-\nu_1^2}{E_1} + \frac{1-\nu_2^2}{E_2}\right)^{-1} \tag{36}$$

The five unknowns in the equations are the deflections $\delta_{\text{x}}, \delta_{\text{y}}, \delta_{\text{z}}$ and the tilting angles $\gamma_{\text{x}}, \gamma_{\text{y}}$. To solve the set of nonlinear Equations 24, for example, the Newton-Raphson method can be used [29]. Initial values for the five unknowns need to be guessed first and the values of r_{q}, r_{p}, a, and K_{p} calculated. To obtain the contact forces for each rolling element Q_{j} and the contact angles α_{j} for the set of Equations 24, the initial values must be inserted into Equation 25 and 26. From there the five unknowns need to be adjusted and the forces and contact angles have to be recalculated in order to converge towards the equilibrium of the set of Equations 24.
Table 2 lists the important bearing geometries and operating parameters for a 6008 and a 6312 deep groove ball bearing, respectively. The load distribution results for the given loads and geometries according to Table 2 are shown in Table 3 and Figure 7. The rolling element at zero degree is in line with in the direction of the radial load and is therefore the highest loaded rolling element.

Table 2
Operational parameters and geometries for a 6008 and 6312 Deep Groove Ball Bearing

Parameter	Value	Unit	Parameter	Value	Unit
6008 - DGBB			6312 - DGBB		
d_{re}	7.938	mm	d_{re}	22.225	mm
$d_{\mathrm{i,groove}}$	8.32	mm	$d_{\mathrm{i,groove}}$	22.5	mm
$d_{\mathrm{o,groove}}$	8.48	mm	$d_{\mathrm{o,groove}}$	22.5	mm
d_{ref}	54	mm	d_{ref}	95	mm
$\alpha_{\mathrm{nominal}}$	0	rad	$\alpha_{\mathrm{nominal}}$	0	rad
P_{d}	0.0039	mm	P_{d}	0.0138	mm
Z	12	–	Z	8	–
n_{i}	2000	1/min	n_{i}	2000	1/min
F_{rad}	500	N	F_{rad}	500	N
F_{ax}	2000	N	F_{ax}	2000	N
ϑ	20	°C	ϑ	20	°C
Lubricant	75W-90	–	*Lubricant*	75W-90	–

Table 3
Calculation results for the presented test case of parameters from Table 2

Parameter	Value	Unit	Parameter	Value	Unit
6008 - DGBB			6312 - DGBB		
δ_{x}	0.00665	mm	δ_{x}	0.00612	mm
δ_{y}	0	mm	δ_{y}	0	mm
δ_{z}	0.13418	mm	δ_{z}	0.09515	mm
γ_{x}	0	rad	γ_{x}	0	rad
γ_{y}	0.00064	rad	γ_{y}	0.0003	rad

3.2. Proportionality factor $\mathrm{k_Q}$

With the contact forces determined with the method presented in Section 3.1 at the inner and outer ring, a proportionality of the individual forces in relation to the total contact force can be established in a similar way to the rolling element capacitance from Equation 21.

$$Q_{\mathrm{ratio,j}} = \frac{Q_{\mathrm{i,j}} \cdot Q_{\mathrm{o,j}}}{Q_{\mathrm{i,j}} + Q_{\mathrm{o,j}}} \cdot \frac{1}{\sum_{\mathrm{j}=1}^{Z} Q_{\mathrm{j}}} \tag{37}$$

with

$$Q_{\mathrm{i,j}} = Q_{\mathrm{o,j}} = Q_{\mathrm{j}} \tag{38}$$

Formula 37 simplifies to

$$Q_{\mathrm{ratio,j}} = \frac{Q_{\mathrm{j}}}{2 \cdot \sum_{\mathrm{j}=1}^{Z} Q_{\mathrm{j}}} \tag{39}$$

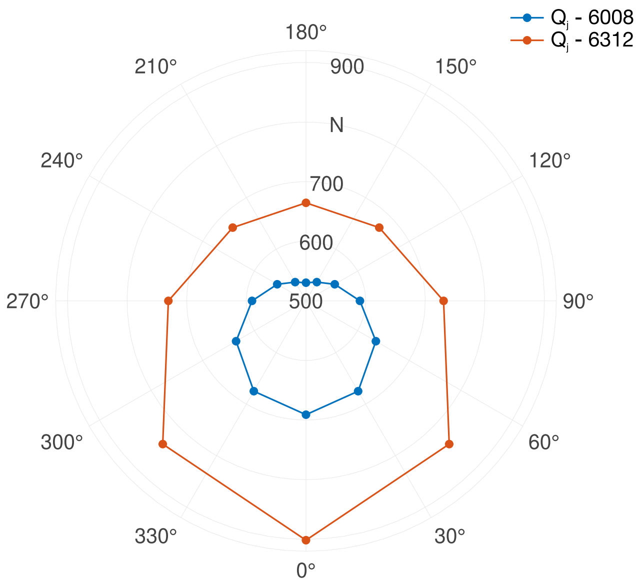

Figure 7: *Load distribution in a 6008 and 6312 DGBB.*

Figure 8 shows the capacitance distribution in a 6008 and 6312 DGBB. A distinction is made between the rolling element-inner ring, -outer ring capacitance and the capacitance of the entire rolling element, which is calculated according to Equation 20. The individual capacitances were calculated according to Equation 5 and 6 using the extended k_C-factor from Equation 16. Using Equation 21 for the capacitance dependent $k_Q(C)$ factor and 39 for the force proportionality Q_{ratio} can be inferred from the calculable values of the capacitance and force distribution. Figure 9 shows both proportionality factors ($k_Q(C)$ and Q_{ratio}) in one graph for each bearing size. A clear correlation between both factors can be seen. The lubricant used is a 75W-90 gear oil described in detail in [10].

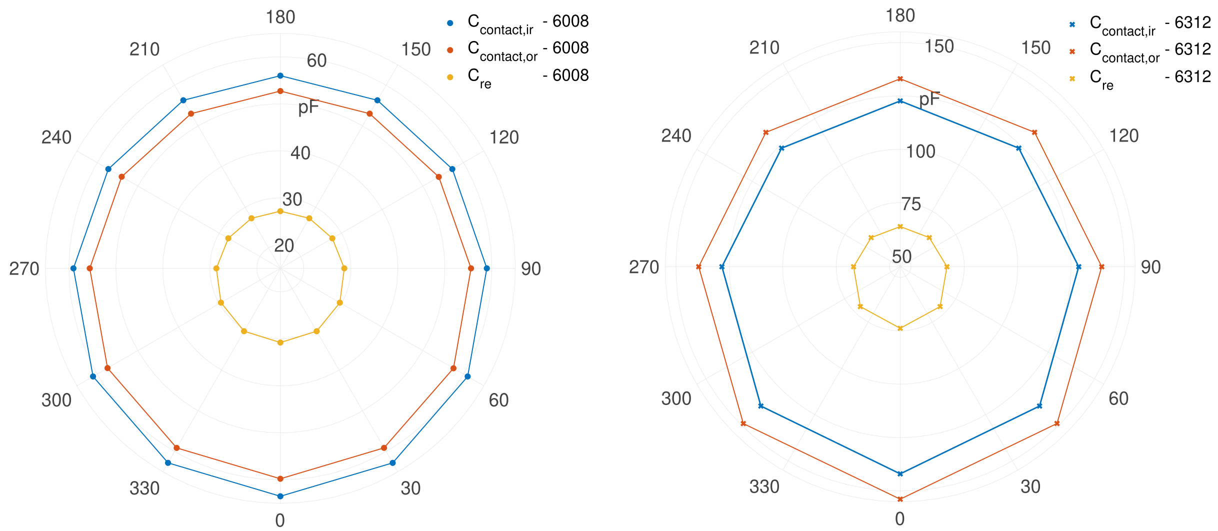

Figure 8: *Capacitance distribution in a 6008 (left) and 6312 (right) DGBB. Please note the different scale values.*

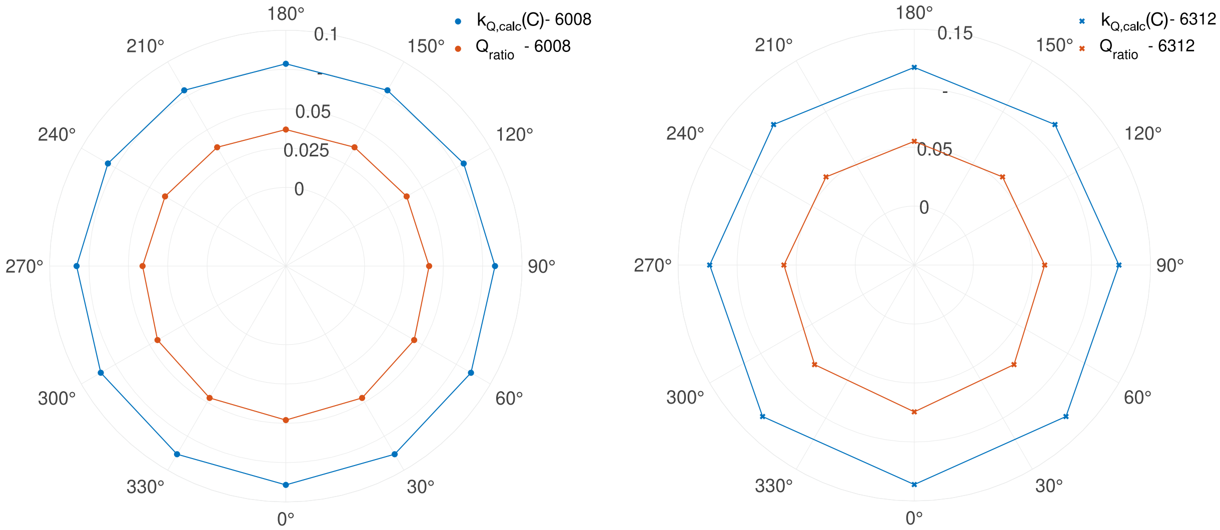

Figure 9: *Capacitance and load ratios in a 6008 (left) and 6312 (right) DGBB. Please note the different scale values.*

It seems to be possible to describe the capacitance proportionality k_Q based on the easily calculable force distribution, since the the trend of both factors shown in Figure 9 shows a clear correlation. However, there is an offset between the two factors that still needs to be considered. As mentioned in section 1, we only consider normal operating speeds. This means that contact angle changes due to centrifugal force influences are neglected. It is therefore assumed that the entrainment velocity $\bar{v}$ at the inner ring and outer ring contact is the same. Therefore, the dimensionless factor U from the HAMROCK-DOWSON EHL-Equations is assumed to be constant. The same applies to the material parameter G. The factors that can vary greatly in a rolling bearing subjected to combined loads are the load (W) and geometrical relationships of the contact (k_e), in particular the osculation in the form of the composite radius $R_{y,Q}$, which is highly variable. The load influence has already been clearly shown in Figure 9. Therefore, it is assumed that the offset could be caused by the osculation $R_{y,Q}$. In order to derive a generally valid formula for different bearing sizes this needs to be considered. Therefore, in addition to the load ratio from Equation 39, a ratio of the composite radii perpendicular to the rolling direction has to be considered as well, which is a measure of the degree of osculation. Since the proportionality factor describes a whole rolling element, consisting of inner- and outer-ring contact, it is necessary to calculate a substitute composite radius for the inner and outer ring contact as described below

$$R_{y,Q} = \frac{R_{y,i} \cdot R_{y,o}}{R_{y,i} + R_{y,o}} \cdot \frac{1}{Z \cdot (R_{y,i} + R_{y,o})} \tag{40}$$

Taking this geometric relationship into consideration, a curve fit factor $k_Q(Q, R_{y,Q})$ was derived based on the calculation of capacitance distributions. This factor is only dependent on the force distribution and the osculation. A system of equations was set up with a large number of individual calculations and a devised equation was optimized using the LEVENBERG-MARQUARDT algorithm [26, 27] from MATLABs *fsolve* function. A first-order optimality of $7.32e-6$ was achieved.

$$k_Q(Q, R_{y,Q}) = Q_{ratio} + 1.5698 \cdot R_{y,Q}^{0.931} + \frac{1 - \sum_{j=1}^{Z} Q_{ratio,j} + 1.5698 \cdot R_{y,Q}^{0.931}}{Z} \tag{41}$$

while

$$\sum_{j=1}^{Z} k_{Q,j}(Q_j, R_{y,Q}) = 1 \tag{42}$$

As it can be seen in Figure 10 both, the load/osculation ratio and the capacitance proportionality are in match. Therefore, it can be said that it is possible to infer the capacitance distribution via the load distribution. For the capacitance-dependent proportionality factor $k_{\mathrm{Q}}(C)$ in Equation 21 and the load-dependent proportionality factor $k_{\mathrm{Q}}(Q, R_{\mathrm{y,Q}})$ in Equation 41, it can be stated

$$k_{\mathrm{Q}}(Q, R_{\mathrm{y,Q}}) = k_{\mathrm{Q}}(C) \tag{43}$$

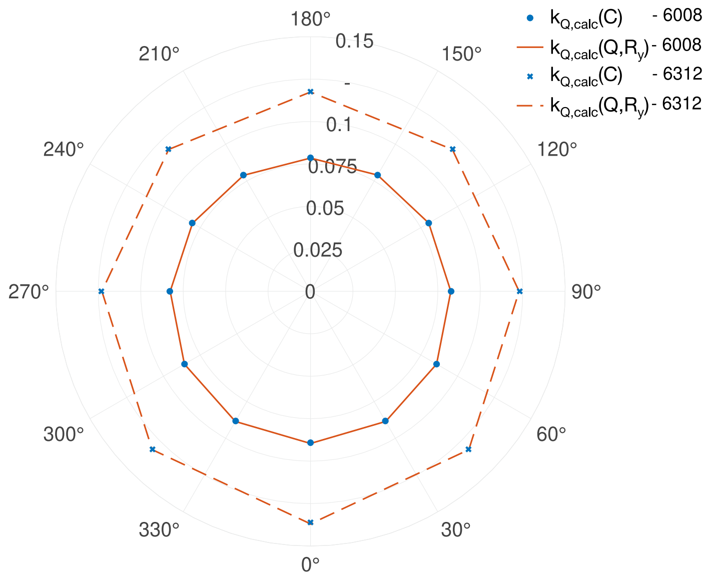

Figure 10: *Ratios of rolling element capacitance $k_{\mathrm{Q}}(C)$ compared to the analytical $k_{\mathrm{Q}}(Q, R_{\mathrm{y,Q}})$-factor for a 6008 and 6312 DGBB.*

3.3. Proportionality factor $\mathbf{k_h}$

The k_{h} factor, introduced by BARZ [4], describes the ratio of the film thickness at the outer ring to the one on the inner ring. For its determination, the entire calculation procedure for film thickness determination must be performed. The presented Equation 44 provides an approach to calculate the k_{h} factor based on the composite radii. Table 4 provides some exemplary calculations for this factor. The factor does not depend on the rotational speed, because effects on the contact angle due to centrifugal forces are not taken into account. Therefor the factor is only influenced by the geometric relations. It ranges roughly from $1.1 < k_{\mathrm{h}} < 1.4$ and is reasonably approximated by the empirical Formula.

$$k_{\mathrm{h}}(R) = \frac{R_{\mathrm{x,i}}}{R_{\mathrm{x,o}}}^{-0.50884} \cdot \frac{R_{\mathrm{y,i}}}{R_{\mathrm{y,o}}}^{0.05025} \tag{44}$$

The differences between the analytical approach from Equation 44, which is easy to use, and the k_{h} factor based on the film thickness determination, which is more complex to calculate, are minimal and affect normal film thicknesses of $0 - 1\mu\mathrm{m}$ only in the single-digit nanometer range.

4. Application to Film Thickness Measurements

Applying the presented methods and formulae, a capacitance measurement can now be used to determine the film thickness of each contact in ball bearings under a combination of an axial and radial load. In order to clarify the procedure, an exemplary case is presented.
Assuming a voltage step of $U_0 = 0.5\,\mathrm{V}$ is applied on one 6206 DGBB with a loading resistance of $R_{\mathrm{L}} = 0.8\,\mathrm{M\Omega}$

Table 4

k_h factor for different operating conditions

Bearing	G_{ir}	G_{or}	U_{ir}	U_{or}	W_{ir}	W_{or}	$k_{e,ir}$	$k_{e,or}$
			2.238e-10	1.719e-10				
6008	4292	4315	4.478e-10	3.439e-10	3.364e-04	1.861e-04	8.1334	5.4568
			6.717e-10	5.159e-10				
			1.377e-10	8.597e-11				
6312	4315	4307	2.754e-10	1.719e-10	6.646e-05	2.561e-05	20.2265	14.9319
			4.131e-10	2.579e-10				

Bearing	$R_{x,i}/R_{x,o}$	$R_{y,i}/R_{y,o}$	$k_{h,calc}$	$k_{h,empirical}$
			1.1905	1.182
6008	0.7442	1.3913	1.1873	1.182
			1.1893	1.182
			1.271	1.275
6312	0.6207	1	1.27	1.275
			1.273	1.275

Table 5

Calculation results for the application example.

Parameter	Value	Unit
δ_x	0.02301	mm
δ_y	0	mm
δ_z	0.14517	mm
γ_x	0	rad
γ_y	0.00261	rad

and a maximum measured voltage of the fully charged capacitor of $U_{max} = 0.3V$. If Equation 11 is used, a resistance value of $R_P = 1.2\,\mathrm{M\Omega}$ is obtained. While analyzing the systems charging response voltage rise, $U_1 = 0.1\,\mathrm{V}$ and $U_2 = 0.2761\,\mathrm{V}$ are determined in a time interval of $\Delta t = 0.4\,\mathrm{ms}$ (comparative to Figure 2). Applying Equation 8 and Equation 9 to those values, a measured total Capacitance of $C_{total} = 392\,\mathrm{pF}$ results. The bearing is lubricated with a 75W-90 gear oil, whose parameters are listed in [10] and is loaded with an axial load of $F_{ax} = 2000\,\mathrm{N}$, a radial load of $F_{rad} = 2000\,\mathrm{N}$ and operated at a temperature of $\vartheta = 21\,°\mathrm{C}$. The radial internal clearance during operation is $P_d = 3.6\,\mathrm{\mu m}$ and the bearing has an inner ring composite radius perpendicular to the rolling direction $R_{y,i} = 0.1949\,\mathrm{m}$ and $R_{y,o} = 0.0881\,\mathrm{m}$ on the outer ring. The 8 rolling elements that orbit the rotational axis at a pitch diameter of 46 mm with 1000 rpm are 11.11 mm in diameter.

When the mentioned parameters are inserted into the load distribution equilibrium specified in subsection 3.1, the deflections and tilting angles shown in Table 5 and the load distribution shown in Figure 11 are obtained.

Table 6
Determined Factors for each rolling element.

RE No.	k_Q	k_h	$k_{C,i}$	$k_{C,o}$	A_i	A_o	$\epsilon_{r,i}$	$\epsilon_{r,o}$
1	0.1632	1.3373	1.5428	1.6560	1.1e-6 m^2	1.14e-6 m^2	2.46	2.46
2	0.1447	1.3373	1.6325	1.7523	9.57e-7 m^2	9.97e-7 m^2	2.46	2.46
3	0.1160	1.3373	1.8419	1.9771	7.18e-7 m^2	7.48e-7 m^2	2.46	2.46
4	0.1051	1.3373	1.9652	2.1093	6.18e-7 m^2	6.44e-7 m^2	2.46	2.46
5	0.1051	1.3373	1.9661	2.1124	6.17e-7 m^2	6.43e-7 m^2	2.46	2.46
6	0.1051	1.3373	1.9652	2.1093	6.18e-7 m^2	6.44e-7 m^2	2.46	2.46
7	0.1160	1.3373	1.8419	1.9771	7.18e-7 m^2	7.48e-7 m^2	2.46	2.46
8	0.1447	1.3373	1.6325	1.7523	9.57e-7 m^2	9.97e-7 m^2	2.46	2.46

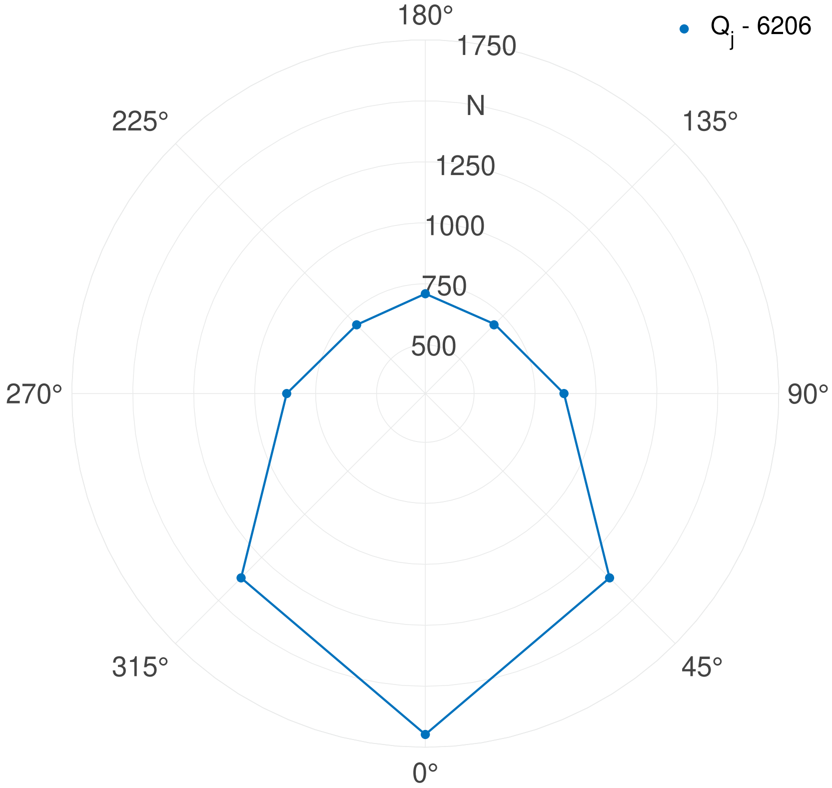

Figure 11: *Load distribution in a 6206 DGBB.*

After obtaining the load of each rolling element it is possible to derive the load proportionality according to Equation 39 and the osculation ratio from Equation 40. The results in turn can be inserted into Equation 41 and the capacitance ratio k_Q can be calculated for each rolling element. The same applies to the film thickness proportionality factor k_h with Equation 44 and the capacitance correction factor k_C with the extended Equation 16. The calculation process is shown in Figure 12 in the form of a flowchart. All important derived factors are summarized in Table 6.

With Equation 22 we calculate the film thickness for the inner ring. The calculation of the film thickness at the outer ring contact uses Equation 15. In the presented case the film thickness of the rolling element subjected to highest load on the inner ring results to 268 nm and on the outer ring to 357 nm.

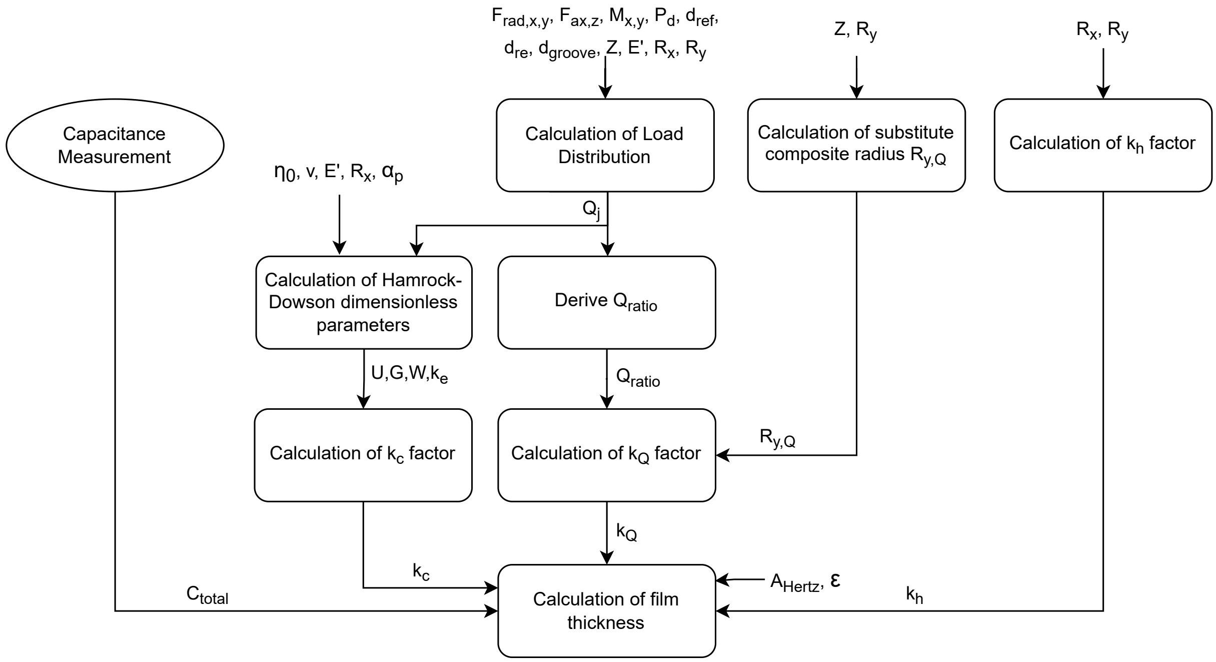

Figure 12: *Flowchart of the film thickness calculation method.*

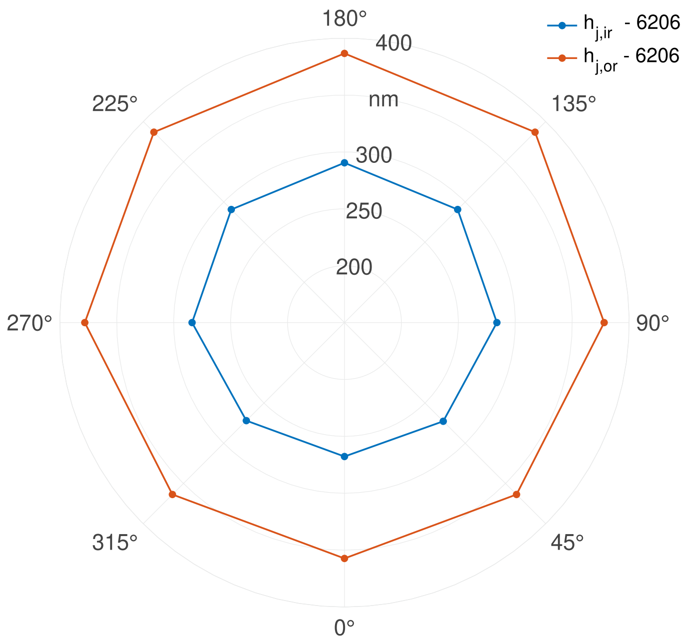

Figure 13: *Calculated Film Thickness Distribution in a 6206 DGBB.*

5. Conclusion and Outlook

This work provides a complete guide from the measurement of electrical bearing capacitance to the derivation of local lubricant film thicknesses of each rolling contact. This includes the basics of measuring a capacitance and determining the capacitance from a voltage step (see section 2) and the calculation of the internal bearing load distribution (see subsection 3.1). A novelty is the method for calculating the local lubricant film thickness of combined loaded point contact bearings. In principle, this method is based on the measured capacitance of the bearing, the calculated load distribution, and osculation. In addition, analytical factors that put these influences in relation were derived. To calculate the proportional capacitance distribution, a correlation between the internal bearing load distribution and osculation were combined into an analytically calculable factor k_Q (see Equation 41). In addition, an analytical formula for the ratio of the lubricant film thickness between the inner and outer ring was derived and merged into a factor k_h (see Equation 44). Furthermore, a revision of the analytical factor k_C (see Equation 16), which was already published in an earlier paper of the authors, was presented. The k_C factor is now adapted for a wider range of applications and can be used for the analytical capacitance calculation of point contact bearing. Finally, an exemplary case is calculated in section 4 to illustrate the principle behind the method.

In future, this method can be extended to purely radially loaded bearings so that the unloaded rolling elements are taken into account [30]. An additional future approach would be the transfer of the presented method from normal speed applications to high-speed applications, by taking the additional influences caused by centrifugal force into account. Furthermore it should be noted that the presented method assumes a quasi-steady state, which neglects the transient damping effects due to film thickness change as a result of an uneven load distribution [31]. Toward larger radial and smaller axial loads, this effect is increased because the contact load on the circumference changes significantly. Therefore, this effect should be considered in future investigations.

Acknowledgements

This work was executed at the Leibniz University Hannover, Germany. The authors would like to thank the "Otto von Guericke"-Research Association (AiF) for their financial support of the project (Grant No. 20496 N).

References

[1] A. Mütze, Bearing Currents in Inverter-Fed AC-Motors, Ph.D. thesis, Technische Universität Darmstadt (2004).

[2] P. Brüser, Untersuchungen über die elastohydrodynamische Schmierfilmdicke bei elliptischen Hertzschen Kontaktflächen, Ph.D. thesis, Technische Universität Carolo-Wilhelmina zu Braunschweig, Braunschweig (1972).

[3] P. Leenders, L. Houpert, Study of the Lubricant Film in Rolling Bearings; Effects of Roughness, in: D. Dowson, C. M. Taylor, M. Godet, D. Berthe (Eds.), Tribology Series, Vol. 11 of Fluid Film Lubrication – Osborne Reynolds Centenary, Elsevier, 1987, pp. 629–638. doi:10.1016/S0167-8922(08)70996-9.

[4] M. Barz, Die Schmierfilmbildung in fettgeschmierten schnellaufenden Spindellagern, Ph.D. thesis, Leibniz Universität Hannover, Hannover (1996).

[5] K. Jablonka, R. Glovnea, J. Bongaerts, Evaluation of EHD films by electrical capacitance, Journal of Physics D: Applied Physics 45 (2012) 385301. doi:10.1088/0022-3727/45/38/385301.

[6] K. Jablonka, R. Glovnea, J. Bongaerts, Quantitative measurements of film thickness in a radially loaded deep-groove ball bearing, Tribology International 119 (2018) 239–249. doi:10.1016/j.triboint.2017.11.001.

[7] T. Maruyama, K. Nakano, In Situ Quantification of Oil Film Formation and Breakdown in EHD Contacts, Tribology Transactions 61 (2018) 1057–1066. doi:10.1080/10402004.2018.1468519.

[8] T. Maruyama, M. Maeda, K. Nakano, Lubrication Condition Monitoring of Practical Ball Bearings by Electrical Impedance Method, Tribology Online 14 (2019) 327–338. doi:10.2474/trol.14.327.

[9] B. J. Hamrock, D. Dowson, Ball Bearing Lubrication: The Elastohydrodynamics of Elliptical Contacts, Wiley, New York, 1981.

[10] V. Schneider, H.-C. Liu, N. Bader, A. Furtmann, G. Poll, Empirical formulae for the influence of real film thickness distribution on the capacitance of an EHL point contact and application to rolling bearings, Tribology International 154 (2021) 106714. doi:10.1016/j.triboint.2020.106714.

[11] L. E. Murch, W. R. D. Wilson, A Thermal Elastohydrodynamic Inlet Zone Analysis, Journal of Lubrication Technology 97 (2) (1975) 212–216. doi:10.1115/1.3452559.

[12] SKF, The SKF Model for Calculating the Frictional Moment, SKF, 2018.

[13] O. Kreil, Einfluss der Oberflächenstruktur auf Druckverteilung und Schmierfilmdicke im EHD-Kontakt, Ph.D. thesis, Technische Universität München (2013).

[14] N. Bader, A. Furtmann, H. Tischmacher, G. Poll, Capacitances and lubricant film thicknesses of grease and oil lubricated bearings, in: STLE Annual Meeting & Exhibition, At Atlanta, Georgia (Ed.), STLE Annual Meeting & Exhibition, Vol. 72, Atlanta, Georgia (US), 2017, pp. 311–314.

[15] N. Bader, H. Liu, B. B. Zhang, G. Poll, Film Thickness Measurements in EHL-Contacts using Capacitance Measurements, in: 46th Leeds-Lyon Symposium on Tribology 2019, 2019.

[16] A. Furtmann, Elektrische Belastung von Maschinenelementen im Antriebsstrang, Ph.D. thesis, Leibniz Universität Hannover (2017).

[17] E. Wittek, M. Kriese, H. Tischmacher, S. Gattermann, B. Ponick, G. Poll, Capacitances and lubricant film thicknesses of motor bearings under different operating conditions, in: I. Staff (Ed.), 2010 XIX International Conference on Electrical Machines, I E E E, 2010, pp. 1–6. doi:10.1109/ICELMACH.2010.5608142.

[18] A. Cameron, R. Gohar, O. A. Saunders, Theoretical and experimental studies of the oil film in lubricated point contact, Proceedings of the Royal Society of London. Series A. Mathematical and Physical Sciences 291 (1427) (1966) 520–536. doi:10.1098/rspa.1966.0112.

[19] H. Cen, P. M. Lugt, Film thickness in a grease lubricated ball bearing, Tribology International 134 (2019) 26–35. doi:10.1016/j.triboint.2019.01.032.

[20] R. Glovnea, M. Furtuna, Y. Nagata, J. Sugimura, Electrical Methods for the Evaluation of Lubrication in Elastohydrodynamic Contacts, Tribology Online 7 (2012) 46–53. doi:10.2474/trol.7.46.

[21] R. S. Heemskerk, K. N. Vermeiren, H. Dolfsma, Measurement of Lubrication Condition in Rolling Element Bearings, A S L E Transactions 25 (4) (1982) 519–527. doi:10.1080/05698198208983121.

[22] E. Wittek, Charakterisierung des Schmierungszustandes im Rillenkugellager mit dem kapazitiven Messverfahren, Ph.D. thesis, Leibniz Universität Hannover, Hannover (2016).

[23] J. E. Franke, Der Einfluß der Schmierfettzusammensetzung auf das tribologische Verhalten schnellaufender Wälzlager, Ph.D. thesis, Universität Hannover (1999).

[24] A. Lubrecht, Numerical solution of the EHL line and point contact problem using multigrid techniques, Ph.D. thesis, University of Twente. Enschede, The Netherlands (1987).

[25] C. H. Venner, Multilevel solution of the EHL line and point contact problems, Ph.D. thesis, University of Twente. Enschede, The Netherlands (1991).

[26] K. Levenberg, A method for the solution of certain non-linear problems in least squares, Quarterly of Applied Mathematics 2 (2) (1944) 164–168. doi:10.1090/qam/10666.

[27] W. Marquardt, E. Dupont, R. Bennett, G. Burrell, An algorithm for least-squares estimation of nonlinear parameters, Jornal of Society for Industrial and Applied Mathematics Vol. 2 (2) (1963) 431–441. doi:10.1137/0111030.

[28] S. Andréason, Theoretische Grundlagen für die Berechnung von mit Kräften und Momenten belasteten Rillenkugellagern, Konstruktion 21 (3) (1969).

[29] P. Deuflhard, Newton Methods for Nonlinear Problems: Affine Invariance and Adaptive Algorithms, no. 35 in Springer Series in Computational Mathematics, Springer, Berlin ; New York, 2004.

[30] T. Schirra, G. Martin, S. Puchtler, E. Kirchner, Electric impedance of rolling bearings - consideration of unloaded rolling elements, Tribology International 158 (2021). doi:10.1016/j.triboint.2021.106927.

[31] B. Zhang, Multigrid Methods for Anisotropic Heterogeneous Material Simulation in Dry and Elasto-Hydrodynamically Lubricated Contacts, Ph.D. thesis, University of Twente (Aug. 2020).